

An Efficient Sensor Based on Anodic Activation of Graphene Oxide for Sensitive and Selective Determination of Dopamine in Blood Serum

Al-Ghafri L.^a, Al-Hatmi N.^a, Joudi S.A.^b and Khudaish E.A.^{*a}

Department of Chemistry, College of Science, Sultan Qaboos University, Box 36, Al-Khodh 123, Oman; ^bUniversity of Waikato, School of Science, Department of Chemistry, Hamilton, New Zealand. *E-mail:ejoudi@squ.edu.om.

ABSTRACT: A native graphene oxide (NGO) prepared by Hummers modified method was used as the template materials for the fabrication of electrochemically oxidative graphene oxide (OGO) onto a glassy carbon electrode (GCE). The fabrication of OGO-GCE proceeded via reversible anodic cycles of previously coated NGO base surface materials. The development of a new aldehyde/alcoholic functional group on OGO-GCE characterized by X-ray photoelectron spectroscopy (XPS) analysis is a marked signal for surface oxygen richness that provokes the cost of (C-C/C-H) hybridized states. The measurements obtained by an electrochemical impedance spectroscopy (EIS) method demonstrated that the conductivity and the rate of electron transfer process at the OGO-GCE have improved substantially. Quantitatively, the estimated rate constant of OGO was 9 times greater than that of that of NGO. Further evidence on the superiority of OGO over NGO was demonstrated by the outstanding analytical performance on the simultaneous determination of ascorbic acid (AA), dopamine (DA) and uric acid (UA) using the differential pulse voltammetry (DPV) technique. The selectivity of the as-prepared OGO sensor for DA quantification in the presence of high concentrations of both AA and UA was achieved successfully with a detection limit ($DL_{3\sigma}$) lowered to 12 nM in comparison to many electrochemical modified surfaces. The proposed method for the construction of OGO sensors could provide a robust sensing platform for the reliable detection of DA in real biological samples. The OGO-GCE sensor showed excellent stability and performance in serum blood analysis with an acceptable recovery percentage of trace DA quantification ranging between 96% and 102%.

Keywords: Oxidative graphene oxide; Anodic pretreatment; Thin film; Dopamine analysis.

بناء كاشف فعال بواسطة الأوكسدة النشطة لأوكسيد الكرافين لغرض التقدير الإنتقائي والحساس لمادة الدوبامين في الدم

لمياء الغافري ونسيبة الحاتمي وصلاح الدين جوده و عماد خديش

الملخص: إن مادة أوكسيد الكرافين المحضر بطريقة هومرس المعدلة قد اعتمدت كمادة أساسية في تطوير مستشعر حساس بواسطة التنشيط الكهروكيميائي على سطح الكربون الزجاجي. أن عملية التصنيع تتم بواسطة الأوكسدة المتعاقبة لأوكسيد الكرافين المطلي على سطح الكربون الزجاجي، مما يساهم في زيادة تركيز مجموعات الأوكسجين الوظيفية. من خلال قياس التحليل السطحي الذي أثبت وجود مجموعة أوكسجين وظيفية جديدة من الألدهايد / الكحول على سطح المادة المصنعة. كذلك أثبتت طرق الطيف الكهروكيميائي أن سرعة انتقال الإلكترونات إزدادت بمقدار 9 مرات للمستشعر المطور و ذلك يؤيد ان الأوكسدة الفعالة لها دور مهم أيضا في زيادة المسافات البينية بين طبقات أوكسيد الكرافين مما يجعل قدرته التوصيلية على مستويات أعلى وأكبر. لقد أثبتت نتائج التحليل الكهروكيميائي المقدر والانتقائية العالية للمستشعر المطور في تقدير تركيز الدوبامين الى حدود دنيا مقترية من 12 نانو- مولار وبوجود كميات كبيرة من حمض الأسكوربيك وحمض اليوريك كمواد بيولوجية متداخلة ومثبطة. لقد أثبت المستشعر المطور أيضا على تقدير الدوبامين في عينات من مصل الدم وصلت الى مستويات عالية، أن الطريقة المقترحة لتحضير المستشعر من الممكن أن توفر منصة قوية لتقدير الدوبامين في عينات بيولوجية حقيقية. في هذا المضمار فان المستشعر أظهر إستقرارية وقدرة تحليل عالية لعينات من الدم مع نسبة إسترداد مئوية عالية تتراوح بين 96% و 102% لمادة الدوبامين .

الكلمات المفتاحية: أوكسيد الكرافين المتأكسد؛ المعالجة الأنودية؛ الأسطح الرقيقة؛ تحليل الدوبامين.



1. Introduction

Dopamine (DA) is an important catecholamine species that exerts significant influence on the central nerves, memory, hormonal and cardiovascular system [1]. It is composed of an amino group attached to the catechol molecular structure and considered as an electrochemically active constituent. Higher or lower concentrations are associated with neurological disorders such as Schizophrenia and Parkinson's diseases [2,3]. Therefore, accurate and rapid quantification of DA in biological samples is a crucial test that requires a highly sensitive and selective analytical method [4-6].

Recently, several analytical approaches and techniques have been used for the DA detection including spectrophotometric methods such as spectrophotometry, chemiluminescence, electro-chemiluminescence, surface-enhanced Raman spectroscopy and colorimetry [7,8]. These approaches were successfully applied for accurate and sensitive DA quantification but require advanced technical expertise and extreme experimental conditions, are expensive and time-consuming, and suffer from sensitivity and selectivity issues [9]. Electrochemical methods integrate microfluidic systems and are used extensively for DA determination in biological samples with the aim of improving selectivity, sensitivity, feasibility and continuous monitoring ability, fast response times and lower detection limits [10,11]. The coexistence of interfering biomolecules such as ascorbic acid (AA) and uric acid (UA) in biological blood and urine samples gives rise to some challenges due to their close oxidation potential to DA [12,13]. Accordingly, substantial efforts were implemented for construction of modified electrodes with active surface materials capable of overcoming possible overlapping electrochemical signals of the above three biological molecules. Therefore, electrochemical sensors have received considerable interest for biological analysis because of their rapid response, high sensitivity and selectivity [14].

Carbon-based materials including graphene derivatives such as graphene oxide (GO) and reduced graphene oxide (RGO) are the constituents of interest for electrode surface modification for their high reactivity, surface area, stability and simple fabrication [15-17]. They are considered as polymeric-like compounds consisting of various oxygenated functionalities [18]. The structure of GO sheet is characterized by the presence of edge and basal planes defined by the nature of existing oxygen functional groups [19]. The edge plane consists mainly of carbonyl and carboxyl groups, which marks its hydrophilicity along with reaction kinetics facility [20]. The basal plane comprises a combination of both hydrophilic (epoxy and hydroxyl groups) and hydrophobic aromatic domains [21]. Moreover, the oxygenated groups are responsible for ease of solvation and surface functionalization [22]. The above unique structure is acknowledged to strongly influence surface communication and hence the observed electrochemical signal [23,24]. Application of graphene-based materials for construction of active sensors is dominated by combining them with other supportive compounds such as organo-metallic complexes and polymers, metal and metal oxide nanoparticles and other hybrid constituents [25-30]. Application of pristine graphene independently as an active sensing materials is not widely applied because of certain disadvantages attributed to surface passivation and slow electrode kinetics [31,32].

The aim of the present work is to fabricate an active surface materials based on oxidative graphene oxide (OGO) via anodic potential excursion of a previously coated NGO film onto a GCE dipped in the buffer background electrolyte. Herein, we present a full study on the electrochemical properties, elemental structure, surface morphology of the proposed sensor (OGO-GCE) along with its catalytic activity on DA analysis.

2. Experimental

2.1 Chemicals and electrodes

Analytical grade DA, AA, UA, potassium ferrihexacyanate ($K_4[Fe(CN)_6]$), potassium ferrihexacyanate ($K_3[Fe(CN)_6]$), graphite powder, sodium nitrate ($NaNO_3$), sulfuric acid (H_2SO_4), potassium permanganate ($KMnO_4$) and hydrogen peroxide (H_2O_2) were purchased from Sigma-Aldrich Chemie, Germany. Potassium orthophosphate (KH_2PO_4) and dipotassium phosphate (K_2HPO_4) were obtained from BDH, UK. A 0.10 M phosphate buffer solution (PBS) with pH 7.28 was made by mixing certain portions of (KH_2PO_4) and (K_2HPO_4) in distilled water and used for all the present electrochemical measurements unless stated otherwise.

All electrochemical measurements were conducted using BAS 50W workstation (Bioanalytical System, West Lafayette, IN, USA) in a three-electrode cell comprised of glassy carbon working electrode (GCE), a platinum coil and $Ag/AgCl/KCl_{(sat.)}$ as counter and reference electrodes, respectively. Prior to each experiment, the GCE was polished sensibly and evenly with alumina slurry (5.0 and 1.0 μm) at a polishing cloth, rinsed thoroughly with distilled water and sonicated for 5 min using (JAC Ultra Sonic, 1505, LABKOREA INC, Korea) to remove possible adsorbed debris and finally rinsed with distilled water.

2.2 Preparation of graphene oxide

The native blended GO material was synthesized from graphite powder according to the modified Hummers method [31]. Briefly, a mixture of 1.2 g graphite, 1.0 g $NaNO_3$ and 46 mL of H_2SO_4 (98%) were placed in an ice bath and carefully stirred. Then 6.0 g potassium permanganate ($KMnO_4$) was added steadily with continuous stirring. The reaction mixture was then placed in a water bath at 35 °C for 1 h to complete the oxidation reaction.

AN EFFICIENT SENSOR BASED ON ANODIC ACTIVATION OF GRAPHENE OXIDE

The developed reaction mixture was diluted with 100 mL of distilled water and its temperature raised to 95°C for 2 h with gentle stirring when the suspended solution turned brown. The brownish suspension was then treated with 30 mL of 30% H₂O₂ to remove the remaining excess amount of KMnO₄. Finally, the residual material produced in the solution mixture was centrifuged at 6000 rpm for 15 min, separated out and washed with distilled water for several times. The obtained black GO paste was dried under vacuum and a suspended blend of (1 mg GO/1 mL distilled water) was prepared for further surface modification.

2.3 Construction of modified electrodes

A modified GCE was prepared by drop casting of 20 µL GO dispersed solution onto a polished and clean GCE. The modified electrode (NGO-GCE) was placed underneath a warm light projector to dryness. The proposed oxidative OGO-GCE was fabricated by electrochemical pretreatment of (NGO-GCE) in PBS (pH = 7.28) induced by 15 reversible voltammetric cycles between 0.0 mV and 1000 mV at 50 mV/s and terminated in the more anodic potential.

2.4 Equipment and techniques

X-ray Photoelectron Spectroscopy (XPS) was performed to study the relative amounts of elemental groups present in the studied samples (Omicron, Germany). The spectra of individual constituents were estimated by fitting the C 1s curve spectra using Gaussian Lorentzian peak shape after background correction with Shirley function in Casa XPS software (Casa Software Ltd, UK). The binding energies were calibrated with respect to adventitious C 1s feature at 284.6 eV.

Electrochemical Impedance Spectroscopy (EIS) was performed with an open circuit potential using Gamry potentiostat (Interface 1000E, USA) with a frequency range between 100 kHz and 1 Hz at amplitude of 5 mV. The EIS experiments were achieved in electrolytic solution composed of 5 mM of [Fe(CN)₆]^{3-/4-} to study the surface modification influence on the electron transfer kinetics. Fitting of the EIS experimental data were accomplished by selecting the Randle's equivalent simple circuit.

Cyclic voltammetry (CV) was employed for surface modification via reversible potentiodynamic cycles. The differential pulse voltammetry (DPV) was utilized as an active electrochemical method for analytical performance examination of modified electrodes.

2.5 Preparation of the real sample

A serum blood sample collected from Sultan Qaboos University Hospital (SQUH, Muscat, Oman) was diluted three times with the PBS (0.1 M of pH = 7.28) and used directly with no further treatment. An aliquot of 5.0 mM DA was diluted 5 times with the serum buffer solution for the standard addition procedure. The electrochemical measurements of DA were achieved using DPV technique. The regression data obtained from the selective determination of DA in the presence of AA and UA in the prepared artificial sample were used to convert the anodic current response of DA real sample into its equivalent DA concentration. Accordingly, the recovery percentage of DA was estimated to evaluate the performance of the proposed sensor.

3. Results and Discussion

3.1 Characterization methods for identification of surface materials

3.1.1 Surface elemental composition using XPS method

The C 1s XPS experimental data are shown in Figure 1, which identifies the chemical structure of NGO (A) and OGO (B) samples, respectively. The binding energy profiles of carbon functional groups with their different atomic percentage in both samples are evidences of composition alteration. The C 1s core level XPS spectrum of NGO illustrated in Figure 1(A) displays five different chemically shifted components of carbon-carbon and carbon-oxygen functionalities. The characteristic bands at 284.0 and 284.6 eV are attributed to the sp² and sp³ hybridized carbon, respectively, with a total concentration of 47.6%. These are followed by a three smaller peaks centered at 287.0 eV (22.7%), 288.5 eV (21.0%) and 290.4 eV (11.4%) emitted from the carbon-oxygen bonding atoms corresponding to epoxy (C-O-C), carbonyl (C=O), and carboxylate (O-C=O) groups, respectively.

On the other hand, the C 1s spectra for the OGO sample presented in Figure 1(B) is fitted with five peaks obtained at 284.6 eV (26.5%), 285.4 eV (22.4%), 286.4 eV (14.6%), 288.7 eV (28.3%) and 290.1 eV (8.2%) corresponding to (C-C/C-H), (C-O/C-OH), (C-O-C), (C=O) and (O-C=O), respectively.

Variation of the full-width half-maximum (FWHM) values corresponding to the functional groups in both surface materials are quite evident. For instance, the (C-H) hybridized peak in the OGO dropped by 40% while the (C-O-C) and (O-C=O) functionalities are larger by two times as all compared to the NGO.

A close inspection of the data demonstrates the appearance of a new oxygenated peak obtained at 285.4 eV belonging to the aldehyde/alcoholic functional group [34]. The generated peak of (C-O/C-OH) in the OGO configuration with 22.4% is a noticeable evidence for a progressive surface modification achieved by anodic pretreatment of NGO. Increasing the surface concentration of oxygenated groups at the cost of sp² and sp³ hybridized components is another evidence of successful fabrication of OGO.

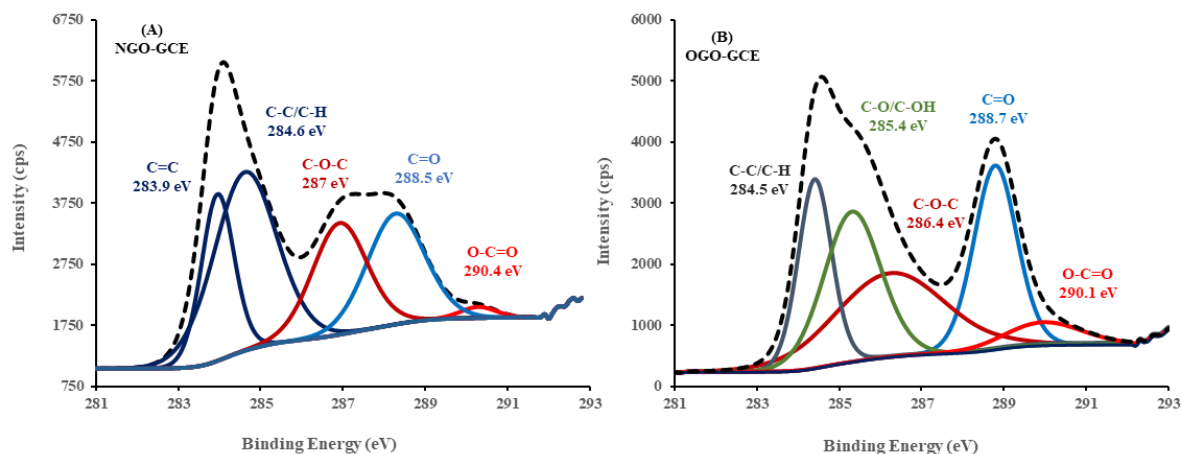


Figure 1. High resolution and curve fitting of C 1s XPS spectra for NGO-GCE (A) and OGO-GCE (B).

3.1.2 Surface interfacial analysis by EIS method

The EIS data for the present two surface modified electrodes were gained under open circuit potential (V_{oc}) in the presence of 5 mM $[\text{Fe}(\text{CN})_6]^{3-/4-}$ solution. A Nyquist plot is a fundamental electrochemical instructive method used to inspect kinetic limitations due to surface modification. As shown in Figure 2, the plot consists of a semicircle curve at high frequency corresponding to the charge transport resistance (R_{ct}) at the electrode/electrolyte interface. The data line at low frequency aligned with the semicircle curve indicates the diffusion-limited process at the active surface materials. Moreover, the non-faradaic process due to uncompensated solution resistance (R_s) is induced by charging of the double layer capacitance (C_{dl}) via the electrostatic attraction of ions at the electrode/electrolyte interface.

Apparently, the gained R_{ct} fitting data for NGO (3250 Ω) is relatively high indicating a surface material of low conductivity that hinders the electron transfer kinetics. At the same time, the Nyquist curve of OGO (inset of Figure 2) is incomparable where the obtained R_{ct} value has dropped markedly to (375 Ω).

The plot suggests a substantial improvement on the surface conductivity and hence the electron transfer kinetics. The electrochemical behavior of NGO before and after anodic treatment shows a major change in the physical properties of doped surface materials, which is influenced by the interlayer distance between graphene layers. The above experimental data demonstrates strong stacking attractions among NGO layers. Nevertheless, the interlayer spacing in OGO were increased by increasing the surface oxygen functionalities during anodic treatment that improves its intrinsic conductivity.

The apparent electron transfer rate constant (k_{app}) evaluated theoretically using equation (1) [35], correspond to OGO and NGO results with values of (2.1×10^{-3} cm/s) and (2.3×10^{-4} cm/s), respectively.

$$R_{ct} = \frac{RT}{F^2 A k_{app} C^*} \quad (1)$$

Obviously, the estimated (k_{app}) value for the OGO-GCE is close to nine times greater than that of NGO indicating remarkable electrode kinetics, surface adsorption capacity and electron shuttling processes.

3.1.3 Surface reactivity using DPV method

Figure 3 shows the reactivity of both surface modified electrodes for the simultaneous determination of AA (500 μM), DA (2 μM) and UA (25 μM) in PBS (pH = 7.28). The characteristic and well-defined three peaks corresponding to the all oxidation species determine the reactivity of both surface materials. The recorded current responses of the three biological molecules with the OGO-GCE are much pronounced and greater than those obtained with NGO-GCE. The remarkable reactivity exhibited by OGO-GCE is apparently associated with the large adsorption capacity offered by the presence of surface-active components that enhance the bonding process [36]. The NGO with large passive surface limits the number of binding sites available for adsorption processes, which results in lower electrochemical responses. The presented data describe the powerful properties of OGO surface materials that facilitates the electrochemical measurements.

In addition, there is evidence relating the reactivity of OGO to the anodic exfoliation of NGO at which the abundance surface oxygen functionalities play a role on enhancement of electrode kinetics. The anodic exfoliation is believed to extend to the interlayer spacing among the NGO sheets, which makes electron shuttling more efficient.

3.2 The analytical performance of OGO-GCE

Selective determination of DA in biological samples is vital for diagnosis of a number of diseases. In addition, DA is biologically present at very low concentration compared to the interfering electroactive species such as AA and UA. Therefore, the analytical performance of the proposed sensor (OGO-GCE) was tested for the quantification of DA in the presence of certain amounts of AA or/and UA in PBS (pH = 7.28) using DPV technique.

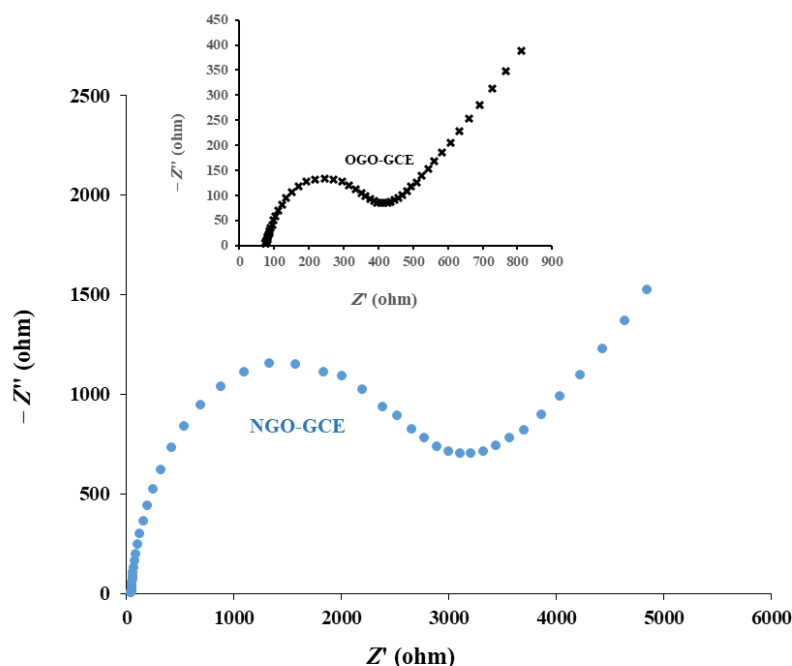


Figure 2. EIS experimental data presented by the Nyquist plot for NGO-GCE. The inset is the data for OGO-GCE.

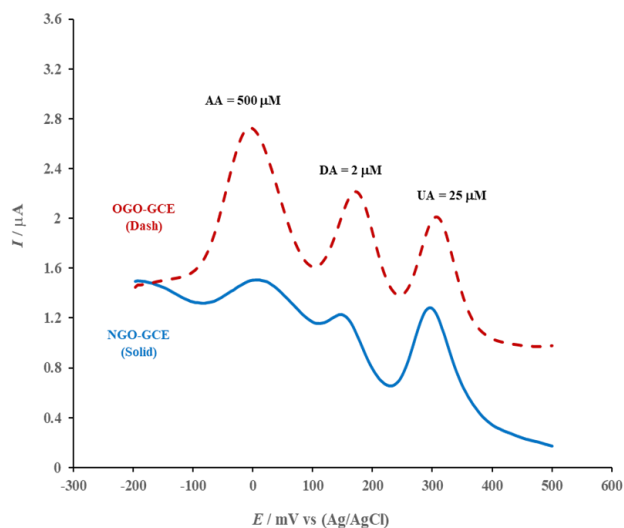


Figure 3. DPV curves of NGO-GCE (blue, solid) and OGO-GCE (red, dashed) towards the simultaneous determination of AA (500 μM), DA (2 μM) and UA (25 μM).

3.2.1 Selectivity test in a binary solution

Figure 4(A) shows the DPV curves for the determination of DA in the presence of 500 μM AA. The dotted line is the current response in the absence of DA where a single anodic peak obtained at 10 mV is characteristic of AA oxidation. With subsequent addition of DA, a new anodic peak arises at 196 mV corresponding to DA oxidation, which increases linearly with each increment of DA concentration. The potential gap (186 mV) between both peak responses is quite reasonable to avoid possible overlap occurring in bare electrodes.

Apparently, the high concentration of AA has no major effect on DA adsorption or electron transfer processes accounted for the electrochemical measurements of DA oxidation. The correlation of peak current (I_p) of DA oxidation to the DA concentration ([DA]) taken from the experimental data given in Figure 4(A) was set up and presented in Figure 4(B).

The regression data of the linear relationship were; $I_p(\mu\text{A}) = 0.5099 (\mu\text{M}) [\text{DA}] + 0.9134 (\mu\text{A})$, which produces a detection limit ($\text{DL}_{3\sigma}$) of 10 nM (DA), where σ is the standard deviation of the background response ($n = 3$) divided by the slope of the linear regression data.

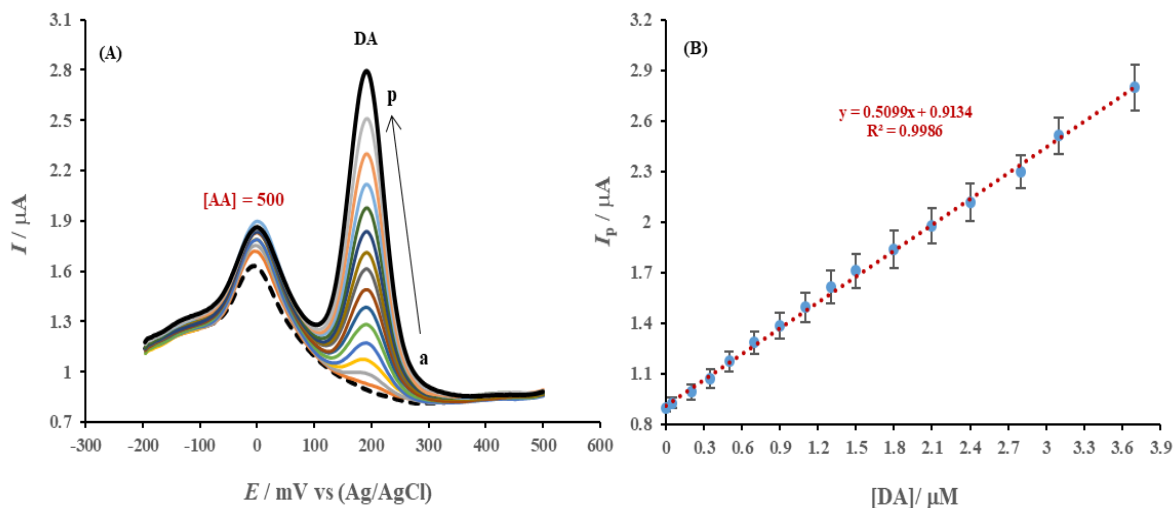


Figure 4. (A) Selective determination of DA in the presence of 500 μM of AA at OGO-GCE in 0.10 M PBS (pH 7.28) using DPV method for a range of [DA] between 0.0 (dotted line, a) and 3.7 μM (solid black, p). (B) The calibration curve plotted as I_p vs [DA] for the data presented in (A) with corresponding error bars.

Figure 5(A) shows the selective determination of DA in the presence of 50 μM UA where the DPV curve in the absence of DA (dotted line) demonstrates the rise of a single anodic peak obtained at 325 mV corresponding to UA oxidation. A new anodic peak current arises by successive addition of small amount of DA obtained at 195 mV due to DA oxidation and increases steadily regardless of the presence of large [UA]. The peak potential separation is 130 mV which is adequate for good identification and assures accurate quantification. The experimental data given in Figure 5(A) were utilized to construct the calibration curve by plotting on the (I_p) of DA versus [DA] as shown in Figure 5(B). The regression data of the linear relationship were; $I_p(\mu\text{A}) = 0.5045 (\mu\text{M}) [\text{DA}] + 1.0054 (\mu\text{A})$, at which the calculated detection limit of DA ($\text{DL}_{3\sigma}$) was 14 nM.

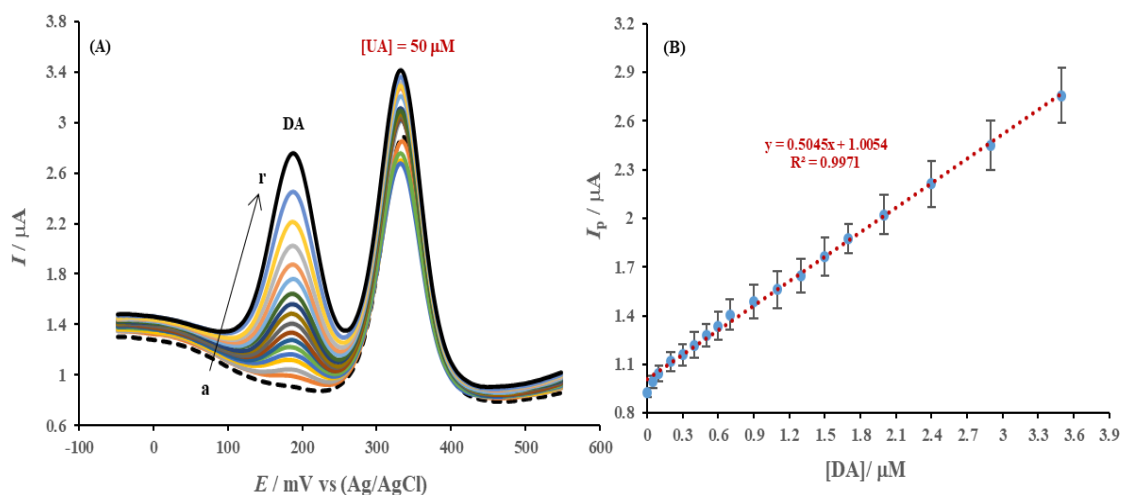


Figure 5. (A) Selective determination of DA in the presence of 50 μM of UA at OGO-GCE in 0.10 M PBS (pH 7.28) using DPV method for a range of [DA] between 0.0 (dotted line, a) and 3.7 μM (solid black, r). (B) The calibration curve plotted as I_p vs [DA] for the data presented in (A) with corresponding error bars.

3.2.2 Selectivity test in a ternary solution

The analytical performance of the proposed sensor for DA detection was examined in an aliquot composed of 500 μM AA and 100 μM UA as shown in Figure 6(A). The dotted line represents the electrode activity in the absence of DA, which results with the appearance of a couple anodic peaks obtained at 15 mV and 335 mV corresponding to AA and UA oxidation, respectively. The addition of DA in small increments produces a well-defined third anodic peak obtained at 195 mV corresponding to DA oxidation, which increases linearly and constantly regardless of the presence of large concentration of the couple interference species. The potential peak-to-peak separation among above studied species exceeds 140 mV, which demonstrates features of merits, robustness and steadiness of the surface materials for sensitive analysis. Figure 6(B) demonstrates the linear (I_p) versus [DA] relationship for the experimental data collected from Figure 6(A). The regression data of the linear relationship were: $I_p(\mu\text{A}) = 0.5056 (\mu\text{M}) [\text{DA}] + 0.8224 (\mu\text{A})$, and the calculated detection limit of DA ($DL_{3\sigma}$) is 12 nM.

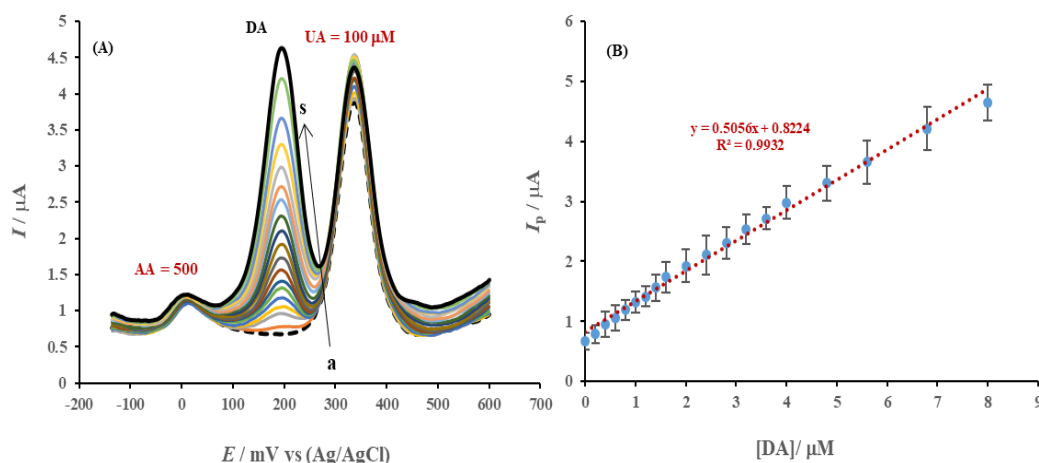


Figure 6. (A) Selective determination of DA in the presence of a binary mixture composed of 500 μM AA and 100 μM UA determined at OGO-GCE in PBS (pH 7.28) using DPV method for a range of [DA] between 0.0 (dotted line, a) and 8.0 μM (solid black, s). (B) The calibration curve plotted as I_p vs [DA] for the data presented in (A) with corresponding error bars.

It is important to note that the standard deviation illustrated by error bars for all data sets presented in the construction of calibration curves shown above were less than 5%. In addition, the slopes of these curves on average have the same value indicating excellent stability and selectivity. Therefore, the overall performance of the present sensor was compared with other applied modified electrodes to summarize its catalytic efficiency as listed in Table 1. The reported detection limit and the sensitivity of the proposed sensor is comparable to or better than the results reported by other relevant surface modified electrodes [37-44]. The above reported results show the importance of the new intended approach on the fabrication of a highly active electrochemical surface characterized by a large surface area and adsorption capacity.

Table 1. The analytical performance of the proposed sensor for DA detection compared to other modified electrodes.

Modified Electrode	DL (μM)	Sensitivity ($\mu\text{A}/\mu\text{M}$)	Reference
PIlox-GO-GCE	0.630	0.211	[37]
ERGO-GCE	0.500	0.482	[38]
PdNPs/GR/CS/GCE	0.100	0.223	[39]
ERGO-P(lysine)-GCE	0.100	0.560	[40]
CNH-P(glycine)-GCE	0.030	0.160	[41]
Ag(hcf)-GR-GCE	0.030	0.133	[42]
Cdots-rGONS-CF	0.020	0.006	[43]
P(glycine)-GO-GCE	0.015	0.534	[44]
OGO-GCE	0.012	0.506	This work

3.3. The stability of the OGO sensor

The reactivity and hence the stability of the proposed sensor was tested by 10 repetitive DPV scans in the presence of 500 μM (AA), 8 μM (DA) and 100 μM (UA). Figure 7 exhibits a negligible drop in the anodic current magnitude of all species. Moreover, the obtained anodic peak potential of the three biological species were consistent and maintained the same peak potential separation. The percent drop of peak current (I_p)% was calculated using equation (2), where $(I_p)_n$ is the peak current at run (n) and $(I_p)_i$ is the initial peak current value at run 1.

$$(I_p)\% = \frac{(I_p)_n}{(I_p)_i} \times 100\% \quad (2)$$

The percent drop in the last run approaches a value of 6%, 4% and 12% of its maxima for AA, DA and UA, respectively, indicating robustness of the solid-state sensor that maintains its reactivity and surface structure environment. The experimental results confirm that the sensor resists poisoning or passivation due to adsorption process of original electroactive molecules and their oxidation byproducts. These unwanted activities are known to deactivate the electrode kinetics associated with weak electrochemical responses.

3.4 Quantification of DA in serum blood

The developed (OGO-GCE) sensor was tested for the determination of DA in serum sample (prepared as described above in the experimental section) using the standard addition method. Figure 8(A) shows a nil current response of serum blood sample as indicated by the dashed line. With subsequent addition of serum-DA aliquot, a well-defined anodic peak was obtained at 192 mV corresponding to DA oxidation, which noticeably increased with each increment. A calibration curve correlates the anodic peak current as a function of [DA] in the range of 0.10 to 2.5 μM as shown in Figure 8(B).

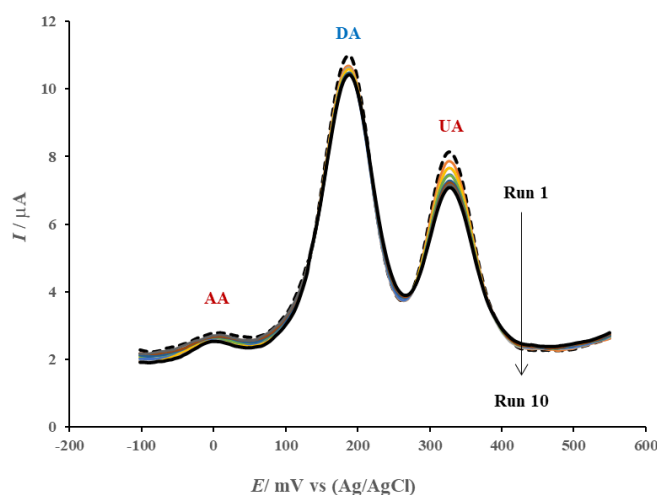


Figure 7. The stability test of the OGO-GCE by repeating the DPV runs from 1 (dotted) to 10 (solid black) in the presence of 500 μM (AA), 8 μM (DA) and 100 μM (UA).

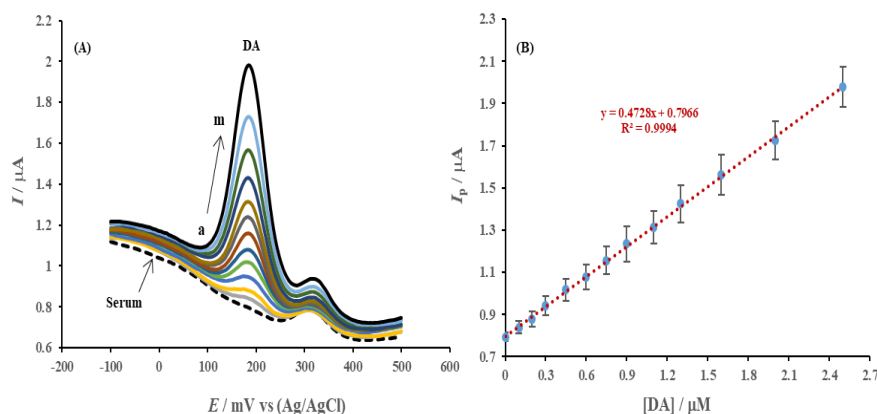


Figure 8. (A) The analytical performance OGO-GCE in the determination of DA in serum blood using standard addition method in PBS (pH 7.28) using DPV method. The [DA] ranged between 0.0 μM (dash black, a) to 2.5 μM (solid black, m). (B) The calibration curve plotted as I_p vs [DA] for the data presented in (A) with corresponding error bars.

3.5 Progress in Neuro-Psychopharmacology and Biological Psychiatry

The regression data are interestingly matching those evaluated above in the sections of selectivity tests. The estimated peak current response in (μA) obtained at 192 mV corresponding to each DA increment was converted into its equivalent concentration in (μM) using the regression data of the calibration curve. Accordingly, the recovery percentages for DA concentrations were calculated ($n = 3$) and summarized in Table 2 along with the relative standard deviation (RSD). The reported recovery values are analytically acceptable which attests to the reliability, stability and robustness of the proposed sensor for accurate DA analysis.

Table 2. The recovery percentage of DA in serum blood sample using standard addition method.

Samples	[Add] (μM)	[Found] \pm RSD ^(a) (μM)	Recovery (%)
(1)	0.00	Not Detected	NA
(2)	0.10	0.097 ± 0.028	96.5
(3)	0.30	0.296 ± 0.027	98.8
(4)	0.60	0.594 ± 0.025	99.0
(5)	0.90	0.915 ± 0.032	101.7
(6)	1.30	1.330 ± 0.027	102.3
(7)	2.50	2.495 ± 0.038	99.8

(a) Relative Standard Deviation ($n = 3$).

7. Conclusion

A steady and simple fabrication approach based on electrochemical oxidative pretreatment of NGO was used to prepare the developed OGO sensor. The exfoliation process of NGO via the anodic activation is expected to increase the interlayer spacing distance between the resultant OGO materials. The conductivity and the rate of electron transfer were substantially increased improving the electrochemical activity of the prepared sensor and hence extending its sensing potential applications. The structure and the catalytic activity of the prepared surface materials were characterized employing various analytical techniques such as XPS, EIS and DPV, all of which have proven the supremacy of OGO over NGO modified electrode. The OGO-GCE sensor showed an outstanding reactivity and stability to the simultaneous and selective determination of DA while lowering the detection limit to 12 nM. The proposed sensor was applied successfully for DA detection in real blood sample with satisfactory results at which the minimum recovery percentage was close to 96.5%.

Conflict of interest

The authors declare no conflict of interest.

Acknowledgment

We would like to thank Sultan Qaboos University (SQU), Sultanate of Oman for supporting this work by the research grant number (IG/SCI/CHEM/18/01). We thank Sultan Qaboos University Hospital (SQUH) for providing serum blood sample.

References

1. Wightman, R.M., May, L.J. and Michael, A.C. Detection of dopamine dynamics in the brain. *Analytical Chemistry* 1988, 60, 769A-779A.
2. Franco, R., Reyes-Resina, I. and Navarro, G. Dopamine in health and disease: Much more than a neurotransmitter. *Biomedicines* 2021, 9, 109 (13 pages).
3. Napier, T.C., Kirby, A. and Persons, A.L. The role of dopamine pharmacotherapy and addiction-like behaviors in Parkinson's disease. *Progress in Neuro-Psycho-pharmacology and Biological Psychiatry* 2020, 102, 109942.
4. Guo, Z., Seol, M-L., Kim, M-S., Ahn, J-H., Choi, Y-K., Liu, J-H. and Huang, X-J., Sensitive and selective electrochemical detection of dopamine using an electrode modified with carboxylated carbonaceous spheres. *Analyst* 2013, 138, 2683-2690.

5. Khudaish, E.A., Al-Nofli, F., Rather, J.A., Al-Hinaai, M., Laxman, K., Kyaw, H.H. and Al-Harthy, S. Sensitive and selective dopamine sensor based on novel conjugated polymer decorated with gold nanoparticles. *Journal of Electroanalytical Chemistry* 2016, **761**, 80-88.
6. Joshi, A., Schuhmann, W. and Nagaiah, T.C. Mesoporous nitrogen containing carbon materials for the simultaneous detection of ascorbic acid, dopamine and uric acid. *Sensors and Actuators B*: 2016, **230**, 544-555.
7. Wang, C., Qi, L. and Liang, R. A molecularly imprinted polymer-based potentiometric sensor based on covalent recognition for the determination of dopamine. *Analytical Methods* 2021, **13**, 620-625.
8. Rostami, A., Hadjizadeh, A. and Mahshid, S. Colorimetric determination of dopamine using an electrospun nanofibrous membrane decorated with gold nanoparticles. *Journal of Materials Science* 2020, **55**, 7969-7980.
9. Ye, F., Feng, C., Jiang, J. and Han, S. Simultaneous determination of dopamine, uric acid and nitrite using carboxylated graphene oxide/lanthanum modified electrode. *Electrochimica Acta* 2015, **182**, 935-945.
10. Kamel, A.H., Amr, A.E., Ashmawy, N.H., Galal, H.R., Al-Omar, M.A. and Sayed, A.Y. Solid-Contact Potentiometric Sensors Based on Stimulus-Responsive Imprinted Polymers for Reversible Detection of Neutral Dopamine. *Polymers* 2020, **12**, 1406(13 pages).
11. Huang, Y., Tang, Y., Xu, S., Feng, M., Yu, Y., Yang, W. and Li, H. A highly sensitive sensor based on ordered mesoporous ZnFe₂O₄ for electrochemical detection of dopamine. *Analytica Chimica Acta* 2020, **1096**, 26-33.
12. Khudaish, E.A., Al-Ajmi, K. and Al-Harthy, S. A solid-state sensor based on ruthenium (II) complex immobilized on polytyramine film for the simultaneous determination of dopamine, ascorbic acid and uric acid. *Thin Solid Films* 2014, **564**, 390 -396.
13. Dey, M.K. and Satpati, A.K. Functionalised carbon nanospheres modified electrode for simultaneous determination of dopamine and uric acid. *Journal of Electroanalytical Chemistry* 2017, **787**, 95-101.
14. Zhang, X., Zhang, Y.C. and Ma, L.X. One-pot facile fabrication of graphene-zinc oxide composite and its enhanced sensitivity for simultaneous electrochemical detection of ascorbic acid, dopamine and uric acid. *Sensors and Actuators B*: 2016, **227**, 488-496.
15. Lee, J., Kim, J., Kim, S. and Min, D.H. Biosensors based on graphene oxide and its biomedical application. *Advanced Drug Delivery Reviews* 2016, **105**, 275-287.
16. Sadak, O. One-pot scalable synthesis of rGO/AuNPs nanocomposite and its application in enzymatic glucose biosensor. *Nanocomposites* 2021, **7**, 44-52.
17. Sireesha, M., Babu, V.J., Kiran, A.S.K. and Ramakrishna, S. A review on carbon nanotubes in biosensor devices and their applications in medicine. *Nanocomposites* 2018, **4**, 36-57.
18. Ye, Z.B., Xu, Y., Chen, H., Cheng, C., Han, L.J. and Xiao, L. A novel micro-nano-structure profile control agent: Graphene oxide dispersion. *Journal of Nanomaterials* 2014, Article ID 582089 (9 pages).
19. Compton, O.C. and Nguyen, S.B. Graphene oxide, highly reduced graphene oxide, and graphene: Versatile building blocks for carbon-based materials. *Small* 2010, **6**, 711-723.
20. Davies, T.J., Moore, R.R., Banks, C.E. and Compton, R.G. The cyclic voltammetric response of electrochemically heterogeneous surfaces. *Journal of Electroanalytical Chemistry* 2004, **574**, 123-152.
21. Brownson, D.A.C., Kampouris, D.K. and Banks, C.E. Graphene electrochemistry: fundamental concepts through to prominent applications, *Chemical Society Reviews* 2012, **41**, 6944-6976.
22. Kuilla, T., Bhadra, S., Yao, D., Kim, N.H., Bose, S. and Lee, J.H. Recent advances in graphene based polymer composites. *Progress in Polymer Science* 2010, **35**, 1350-1375.
23. Power, A.C., Gorey, B., Chandra, S. and Chapman, J. Carbon nanomaterials and their application to electrochemical sensors: a review. *Nanotechnology Reviews* 2018, **7**, 19-41.
24. Silva, A.D., Paschoalino, W.J., Damasceno, J.P.V. and Kubota, L.T. Structure, properties, and electrochemical sensing applications of graphene-based materials. *ChemElectroChem* 2020, **7**, 4508-4525.
25. Vinodh, Kumar, G., Ramya, R., Potheher, I.V., Vimalan, M. and Peter, A.C. Synthesis of reduced graphene oxide/Co₃O₄ nanocomposite electrode material for sensor application. *Research on Chemical Intermediates* 2019, **45**, 3033-3051.
26. Li, G., Zhong, P., Ye, Y., Wan, X., Cai, Z., Yang, S., Xia, Y., Li, Q., Liu, J. and He, Q. A highly sensitive and stable dopamine sensor using shuttle-like α -Fe₂O₃ nanoparticles/electro-reduced graphene oxide composites. *Journal of Electrochemical Society* 2019, **166**, B1552-B1561.
27. Al-Graiti, W., Foroughi, J., Liu, Y. and Chen, J. Hybrid graphene/conducting polymer strip sensors for sensitive and selective electrochemical detection of serotonin. *American Chemical Society Omega* 2019, **4**, 22169-22177.
28. Khudaish, E.A., Myint, M.T.Z. and Rather, J.A. A solid-state sensor based on poly(2,4,6-triaminopyrimidine) grafted with electrochemically reduced graphene oxide: Fabrication, characterization, kinetics and potential analysis on ephedrine. *Microchemical Journal* 2019, **147**, 444-453.
29. Gorle, D.B. and Kulandainathan, M.A. Electrochemical sensing of dopamine at the surface of a dopamine grafted graphene oxide/poly(methylene blue) composite modified electrode. *Royal Society of Chemistry Advances* 2016, **6**, 19982-19991.
30. Li, J., Wang, Y., Sun, Y., Ding, C., Lin, Y., Sun, W. and Luo, C. A novel ionic liquid functionalized graphene oxide supported gold nanoparticle composite film for sensitive electrochemical detection of dopamine. *Royal Society of Chemistry Advances* 2017, **7**, 2315-2322.

31. Liu, Q., Ma, R., Du, A., Zhang, X., Fan, Y., Zhao, X., Zhang, S. and Cao, X. Investigation on structure and corrosion resistance of complex inorganic passive film based on graphene oxide. *Corrosion Science* 2019, **150**, 64-75.
 32. Su, Y., Kravets, V.G., Wong, S.L., Waters, J., Geim, A.K. and Nair, R.R. Impermeable barrier films and protective coatings based on reduced graphene oxide. *Nature Communications* 2014, **5**, 4843-4845.
 33. Khudaish, E.A. and Al-Khodouri, A. A surface network based on reduced graphene oxide/gold nanoparticles for selective determination of norepinephrine in real samples. *Journal of Electrochemical Society* 2020, **167**, 146516.
 34. Gengenbach, T.R., Major, G.H., Linford, M.R. and Easton, C.D. Practical guides for x-ray photoelectron spectroscopy (XPS): Interpreting the carbon 1s spectrum. *Journal of Vacuum Science and Technology A*: 2021, **39**, 013204.
 35. Bard, A.J. and Faulkner, L.R. *Electrochemical Methods: Fundamentals and Applications*, Wiley, New York, Second Edition, 2001.
 36. Brownson D.A.C., Gómez-Mingot M. and Banks C.E., CVD graphene electrochemistry: biologically relevant molecules. *Physical Chemistry Chemical Physics* 2011, **13**, 20284-20288.
 37. Liu, X.F., Zhang, L., Wei, S.P., Chen, S.H., Ou, X. and Lu, Q.Y. Over-oxidized polyimidazole-graphene oxide copolymer modified electrode for the simultaneous determination of ascorbic acid, dopamine, uric acid, guanine and adenine. *Biosensors and Bioelectronics* 2014, **57**, 232-238.
 38. Yang, L., Liu, D., Huang, J. and You, T. Simultaneous determination of dopamine, ascorbic acid and uric acid at electrochemically reduced graphene oxide modified electrode. *Sensors and Actuators B*: 2014, **193**, 166-172.
 39. Wang, X., Wu, M., Tang, W., Zhu, Y., Wang, L., Wang, Q., He, P. and Fang, Y. Simultaneous electrochemical determination of ascorbic acid, dopamine and uric acid using a palladium nanoparticle/graphene/chitosan modified electrode. *Journal of Electroanalytical Chemistry* 2013, **695**, 10-16.
 40. Zhang, D., Li, L., Ma, W., Chen, X. and Zhang, Y. Electrodeposited reduced graphene oxide incorporating polymerization of l-lysine on electrode surface and its application in simultaneous electrochemical determination of ascorbic acid, dopamine and uric acid. *Materials Science and Engineering C*: 2017, **70**, 241-249.
 41. Zhang, G., He, P., Feng, W., Ding, S., Chen, J., Li, L., He, H., Zhang, S. and Dong, F. Carbon nanohorns/poly(glycine) modified glassy carbon electrode: Preparation, characterization and simultaneous electrochemical determination of uric acid, dopamine and ascorbic acid. *Journal of Electroanalytical Chemistry* 2016, **760**, 24-31.
 42. Zhang, F., Li, S., Zhang, H. and Li, H. A Silver Hexacyanoferrate-Graphene Modified Glassy Carbon Electrode in Electrochemical Sensing of Uric Acid and Dopamine. *International Journal of Electrochemical Science* 2017, **12**, 11181-11194.
 43. Fang, J., Xie, Z., Wallace, G. and X. Wang. Co-deposition of carbon dots and reduced graphene oxide nanosheets on carbon-fiber microelectrode surface for selective detection of dopamine. *Applied Surface Science* 2017, **412**, 131-138.
 44. He, S., He, P., Zhang, X., Zhang, X., Liu, K., Jia, L. and Dong, F. Poly(glycine)/graphene oxide modified glassy carbon electrode: Preparation, characterization and simultaneous electrochemical determination of dopamine, uric acid, guanine and adenine. *Analytica Chimica Acta* 2018, **1031**, 75-82.
-

Received 4 April 2023

Accepted 28 May 2023